Available online at www.sciencedirect.com

ScienceDirect

Procedia Chemistry 1 (2009) 883–886

Procedia Chemistry

www.elsevier.com/locate/procedia

Proceedings of the Eurosensors XXIII conference

Single stage deflection amplification mechanism in a SOG capacitive accelerometer

I. Zeimpekis*, M. Kraft

University of Southampton, Southampton, United Kingdom

Abstract

This work discusses on a novel mechanical amplification concept for micro-electro-mechanical systems (MEMS). A single stage deflection amplifying mechanism, comprising microlevers, is implemented for a single axis in-plane capacitive accelerometer. Such a mechanism can provide a higher signal to noise ratio in a wide bandwidth with improved performance. Results from the analysis and evaluation of the fabricated prototype sensor are presented in this paper.

Keywords: mechanical amplification; microlevers; capacitive accelerometer; leverage mechanism

1. Introduction

Due to the difficulties in realizing rigid-links (i.e. bearings) in (MEMS), compliant mechanisms [1], such as flexible beams, are used to suspend structures and provide mobility along desired directions. This work proposes a mechanical amplification scheme that employs microlevers to amplify deflection.

Mechanical amplification mechanisms have already been used in previous studies for various micromachined systems [2-5]. However there have been only a few studies on the application of such mechanisms in inertial sensors [7-9]. This paper presents the results on analysis, design and evaluation of a deflection amplification mechanism implemented in a capacitive accelerometer.

2. Mechanical amplification

Since capacitive inertial sensors rely on displacement to produce an output, their sensitivity is limited by the amplitude of the deflection of their sensing elements along the sense axis. Achieving a higher deflection by amplifying it, improves the output signal level, thereby reducing the gain requirements for the interface circuit. This effectively results in a reduced noise floor since the mechanical amplifier does not actively add noise unlike electronic signal amplification. With this approach a higher signal-to-noise ratio (SNR) can therefore be achieved compared to a conventional accelerometer as depicted in Fig. 1.

* Corresponding author. Tel.: +44-(0)23-8059-3126.
E-mail address: izk07r@ecs.soton.ac.uk.

doi:10.1016/j.proche.2009.07.220

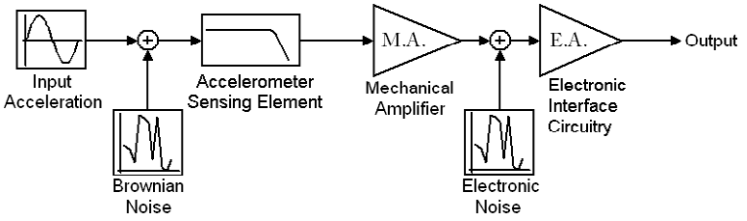

Fig. 1. Block diagram of an accelerometer implemented with a mechanical amplification stage. Where M.A. and E.A are the mechanical and electronic amplifications respectively.

2.1. Microlevers

The amplification mechanism presented here comprises microlevers to achieve deflection amplification. Out of the three types of microlevers available, type 3 microlevers can amplify deflection and their geometry is suitable for implementing them with a sensing element [10]. An analytical model for type 3 microlevers can be extracted by using the individual stiffness of its flexible members and by employing a free-body diagram and the method of superposition. Fig. 2 shows a model of a type 3 microlever assuming a perpendicular to the input force F (following force) with negligible horizontal forces. Pivot, input link, and arm are assumed to be rigidly connected so that the angle at their intersection points is always 90 degrees. In this model the pivot has been substituted by a torsional and an axial spring while the bending of the arm is also taken into consideration.

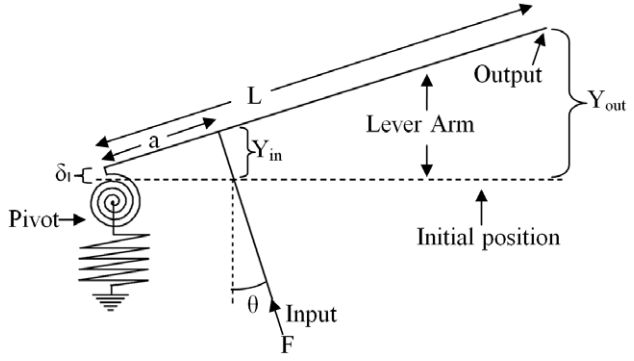

$$A_d = \frac{Y_{out}}{Y_{in}} = \frac{Y_{prout} + \delta_l + D_{aout}}{Y_{prin} + \delta_l + D_{ain}} =$$

$$= \frac{L \cdot \sin(\theta) + \dfrac{F \cdot l}{A \cdot E} + \dfrac{F \cdot a^2 \cdot \left[2 \cdot a + 3 \cdot (L - a)\right]}{6 \cdot E \cdot Ia}}{a \cdot \sin(\theta) + \dfrac{F \cdot l}{A \cdot E} + \dfrac{F \cdot a^3}{3 \cdot E \cdot Ia}} \quad (1)$$

Fig.2 Model of a type three microlever

In an ideal lever the deflection amplification factor would be the ratio of the output to pivot over the input to pivot distance. Since microlevers use flexible members that store energy the amplification factor is not ideal (A_d) and is extracted through the analysis. In eq. 1 the ratio between the output and input deflection is constructed using the rotational and axial deflection of the pivot (Y_{pout}, Y_{prin}, δ_l) and the bending deflection of the arm (D_{aout}, D_{ain}) for the output and the input respectively. The pivot in the model is of length l with an area of cross section A. E is the Young's Modulus and I_a the moment of inertia of the arm. The analytical model of Eq. 1 was compared to FEM simulation models and the deviations between the results were smaller than 0.1 % in the linear region.

2.2. Deflection amplification in a capacitive accelerometer

In order to investigate the concept after the evaluation of the individual microlevers a system of type 3 microlevers was implemented in a single axis capacitive accelerometer. Fig. 3 shows a schematic model of the designed accelerometer, this comprises a proof-mass (a), four symmetrically arranged amplifying microlevers (b), and three differential comb-finger stages for read-out and force-feedback control. Comb-finger stage (c) at the end of the microlevers provides the amplified output to the pick-off circuit. Comb-finger stage (d) on the proof mass is used for force-feedback and stage (e) can be used for comparative signal pick-off. The microlevers also act as the suspension system of the proof mass. The entire structure is anchored to the substrate at points (f).

The operation of the accelerometer is as follows. When the sensor is subjected to acceleration along its sensitive axis (Y-Axis in Fig. 3) the proof-mass is displaced along the same axis. This motion is amplified and transferred to the output, through the microlevers. Each pair of microlevers has its output connected to a differential comb-finger stage, where the amplified motion can be electronically picked-off. This configuration allows amplification of the proof-mass deflection through the microlevers, with a ratio defined by the design geometry parameters. The deflection amplification factor (deflection at the output comb-fingers over the deflection at the centre of the proof-mass) was designed to be 66. The natural frequency along Y-axis is 346 Hz, and the deflection-bandwidth product is 913 μm·Hz. The latter may be used as a figure of merit for comparison with other accelerometers.

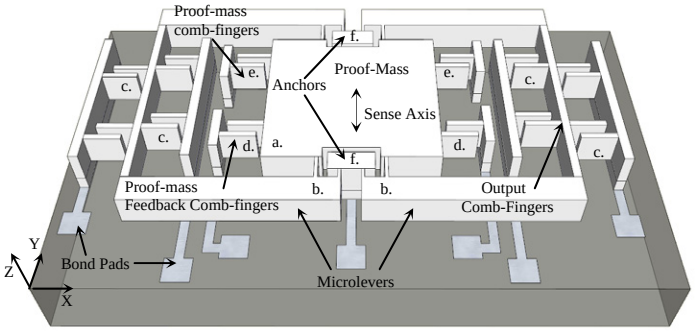

Table 1. Specifications of the accelerometer

Property	***Value***
Die area	6.64x5(mm)^2
Proof Mass	3.08 mg
Proof-mass deflection for 1G	4.03e-2 μm
Comb-fingers' deflection for 1G	2.64 μm
Deflection amplification	66
Input stiffness	738.61 N/m
Output stiffness	11.26 N/m
Resonance frequency	346 Hz
Nominal capacitance	22.94 pF
Static sensitivity	9.5 pF/G
1G Deflection-BW product	913.44 μm·Hz

Figure 3. Schematic of the single stage mechanically amplified capacitive accelerometer showing. a. Proof-mass, b. Microlevers, c. Output comb-fingers, d. Proof-mass feedback comb-fingers, e. Proof-mass comb-fingers, f. Anchors.

2.3. Evaluation of the mechanically amplified capacitive accelerometer

Table 1 presents the specifications of the sensors achieved through optimization by using analytical models and FEM simulations. The model used for the FEM simulations is shown in Fig. 4, with results for 1g acceleration from the commercial software Coventorware. Since comb-fingers render the simulations computationally intensive those were lumped on the proof-mass and the output mechanism of the accelerometer model.

The amplified accelerometers are currently being evaluated in the Polytec's MSA-400 optical measurements system which does not require pick-off electronics. The effective fabrication of the structures was validated using white light interferometry, while their operation using stroboscopic image correlation (Fig. 5). Fig. 6 shows a comparison measurement between the proof-mass and output displacement of the accelerometer. To obtain this diagram the sensor was driven with a sinusoidal signal of 13 HZ at 12 V and a bias voltage of 3 V. Although the proof-mass deflection lies in the noise floor region of the measurement equipment it is evident from the graph that the mechanical amplification for the tested sensor is close to the expected value.

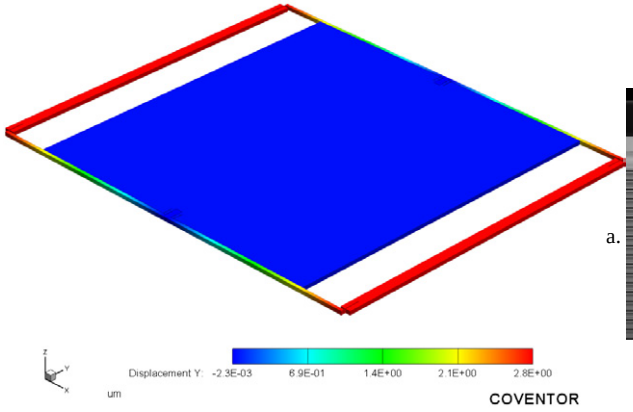

Fig. 4 FEM model and output deflection from Coventorware

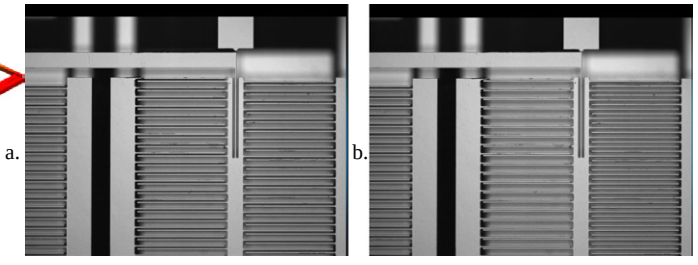

Fig.5 a. Initial position b. maximum deflection of the output of the sensor

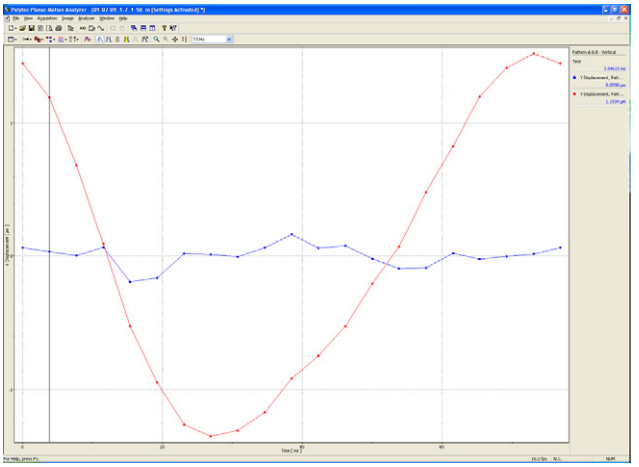

Figure 6. Input/Output displacement comparison

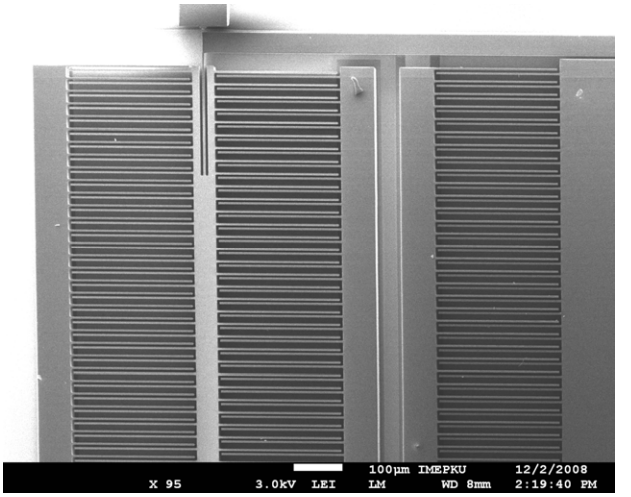

Figure 7. SEM detail from the output mechanism of the accelerometer

3. Fabrication

The sensors were fabricated by employing a three mask Silicon on Glass (SoG) process. The anchor areas were formed on the backside of the highly doped silicon wafers by DRIE etching. The depth of the backside etching is 20µm providing a low squeeze film damping with the substrate. The backside was also doped by phosphorous ions implantation for good ohmic contact. A 200nm thick Ti/Pt/Au layer is patterned by lift off on the Pyrex 7740 wafers to form the electrical interconnections. The two wafers were anodically bonded. The structural layer was formed by thinning the front side using KOH leaving in this way a 60 µm thick layer. Finally the structures were formed by an ICP DRIE etching. Fig. 7 presents an SEM image of the output mechanism and part of the proof-mass of the sensor.

4. Conclusions

The application of mechanical amplification in inertial sensors is evaluated through this work. The results from simulations as well as from the characterization of the fabricated prototype sensors show that the scheme of mechanical amplification can be effectively introduced to enhance the performance of MEMS. Since the mechanical amplifier does not introduce noise to the system, its use can improve the noise figures of inertial sensors without requiring a complicated fabrication process. Further evaluation will reveal structural improvements that can be applied to optimize the use of microlever based amplification mechanisms in capacitive accelerometers and MEMS in general.

References

1. Howell LL, Compliant Mechanisms, New York, 2001, John Wiley & Sons
2. Tsai JC and Ming WC, Journal of Micromechanical Systems 2006, vol. 15, no. 5, pp. 1209-1213
3. Shen X, Zhang Y and Chen X, Nano/Micro Engineered and Molecular Systems, NEMS 2006, pp. 1025-1028
4. Chen TL and Horowitz R, Proceedings of the American Control Conference 2001, vol. 2, pp. 1235-1240
5. Kim C and Kota S, Proceedings of DETC 2002.
6. Tantanawat T, Li Z and Kota S, Proceedings of DETC 2004.
7. Su X-P S and Yang HS, Journal of Structural and Multidisciplinary Optimization 2001, vol. 21. no. 3, pp. 246-252
8. Su X-P S, Yang HS, Journal of Structural and Multidisciplinary Optimization 2001, vol. 22. no. 4, pp. 328-334
9. Claus BW, Pedersen and Ashwin A Sheshia, J. Micromech. Microeng. 2004, vol. 14, pp. 1281-1293
10. Zeimpekis I, Kraft M, MME 2008, vol. 19, pp. 291-294